Journal of Nuclear Medicine, published on September 22, 2016 as doi:10.2967/jnumed.116.181800

Imaging Response to Androgen Receptor Inhibition Using ^{68}Ga-PSMA-11 PET: First Human Experience

Thomas A. Hope, MD,[1,2,3] * Charles Truillet, PhD,[1] * Eric C. Ehman, MD,[4] Ali Afshar-Oromieh, MD,[5] Rahul Aggarwal, MD,[3,6] Charles J. Ryan, MD,[3,6] Peter R. Carroll, MD,[3,7] Eric J. Small, MD,[3,6] and Michael J. Evans, PhD[1]

* co-first authors

1. Department of Radiology and Biomedical Imaging, University of California, San Francisco, San Francisco, CA
2. Department of Radiology, San Francisco VA Medical Center, San Francisco, CA
3. Helen Diller Family Comprehensive Cancer Center, University of California, San Francisco, San Francisco, CA
4. Department of Radiology, Mayo Clinic, Rochester, MN
5. Department of Nuclear Medicine, Heidelberg University Hospital, Heidelberg, Germany
6. Division of Hematology/Oncology, Department of Medicine, University of California, San Francisco, San Francisco, CA
7. Department of Urology, University of California, San Francisco, San Francisco, CA

Running title: AR inhibition effect on PSMA PET

Grant support: T.A.H. was supported by the Radiological Society of North America and the Department of Radiology and Biomedical Imaging, UCSF. M.J.E. was supported by the 2013 David H. Koch Young Investigator Award from the Prostate Cancer Foundation, the National Institutes of Health (R00CA172695, 1R01CA17661), a Department of Defense Idea Development Award (PC140107), the UCSF Academic Senate, and GE Healthcare. C.T. was supported by a postdoctoral fellowship from the Department of Defense Prostate Cancer Research Program (PC151060). Research from UCSF reported in this publication was supported in part by the National Cancer Institute of the National Institutes of Health under Award Number P30CA082103.

Word count: 2,711

Submission type: Brief Communication

Co-Corresponding Authors:

Thomas A. Hope, MD
505 Parnassus Avenue – 0628
Department of Radiology and Biomedical Imaging
University of California, San Francisco
San Francisco, CA 94143-0628
Phone: (415) 353-1905
Email: thomas.hope@ucsf.edu

Michael J. Evans, PhD
185 Berry Street, Lobby 6, Ste. 350
Department of Radiology and Biomedical Imaging
University of California, San Francisco
San Francisco CA 94107
Phone: (415) 353-3442
Email: michael.evans@ucsf.edu

Abstract

Purpose: To evaluate the effect of androgen receptor (AR) inhibition on Prostate Specific Membrane Antigen (PSMA) uptake imaged using ^{68}Ga-PSMA-11 Positron Emission Tomography (PET) in a mouse xenograft model and in a patient with castration sensitive prostate cancer.

Procedures: We imaged three groups of four mice bearing LNCaP-AR xenografts before and seven days after treatment with ARN-509, orchiectomy and control vehicle. Additionally, we imaged one patient with castration sensitive prostate cancer before and four weeks after treatment with androgen deprivation therapy (ADT). Uptake on pre- and post-treatment imaging was measured and compared.

Results: PSMA uptake increased 1.5 to 2.0 fold in the xenograft mouse model after treatment with both orchiectomy and ARN-509, but not with vehicle. Patient imaging demonstrated a seven-fold increase in PSMA uptake after the initiation of ADT. 13 of 22 lesions in the imaged patient were only visualized on PSMA PET after treatment with ADT.

Conclusions: Inhibition of the AR can increase PSMA expression in prostate cancer metastases and increase the number of lesions visualized using PSMA PET. The effects seen in cell and animal models can be recapitulated in humans. Further work needs to be done to better understand temporal changes of PSMA expression in order to leverage this effect for both improved diagnosis and therapy.

INTRODUCTION

Prostate Specific Membrane Antigen (PSMA) is a 100-kD transmembrane glycoprotein which is over expressed on nearly all prostate cancers, particularly poorly differentiated and metastatic lesions (*1-3*). During the past two years the literature contains over 1,000 patients imaged using PSMA-ligands, which have focused on the ability to detect metastases in patients with biochemical recurrence, demonstrating an improved detection rate compared to choline PET or other conventional imaging modalities (*4-9*).

Unlike fluorodeoxyglucose, PSMA expression is not positively correlated with disease progression. In fact, cellular PSMA expression is regulated by the androgen receptor (AR), which is frequently targeted during prostate cancer treatments and can therefore confound interpretation. Opposite of PSA levels, PSMA expression on the cell surface increases with AR inhibition (*10-12*). Previous work by Evans et al in mice bearing PSMA expressing xenografts demonstrated that PSMA expression is increased with both orchiectomy and enzalutamide (*11*), which has recently been reproduced in multiple prostate cancer cell lines and circulating tumor cells (*13,14*).

We hypothesize that inhibition of the AR will result in a transient increase in PSMA expression on prostate cancer cells. First we evaluated the effect of AR targeted therapies in a xenograft model using ^{68}Ga-PSMA-11. Second, since over 90% of patients initially respond to androgen deprivation therapy (ADT), we chose a patient with castration sensitive metastatic disease as an in vivo test of our hypothesis that AR inhibition will increase PSMA expression (*15*).

MATERIALS AND METHODS

Labeling Procedure of ^{68}Ga-PSMA-11

^{68}Ga was obtained by eluting a ^{68}Ge/^{68}Ga generator (iTG) yielding radioactivity in the range of 15 to 30 mCi during synthesis. The syntheses were conducting using iQS® Ga-68 Fluidic Labeling Module. Precursor (DKFZ-PSMA-11) or Glu-NH-CO-NH-Lyx(Ahx)-HBED-CC where HBED-CC = (N,N'-Bis[2-hydroxy-5-(carboxyethyl)-benzyl]ethylenediamine-N-N'-diacetic acid, was purchased from ABX Advanced Biochemical Compounds (Radeberg, Germany). All reagents for formulating final product were provided in a kit from ABX.

Precursor was dispensed into 5 ug aliquots dissolved in 100 uL of 0.25M sodium acetate buffer and stored in -20C freezer until use. The precursor (made up to a total of 1mL with sodium acetate buffer) was added to the preheated reaction vessel (100-110C) and the generator is immediately eluted into the reaction vessel. The contents were heated for 5 minutes after which they were pushed through an activated C18 seppak lite cartridge and the contents were directed to a waste vial. The reaction vessel was further washed with 5mL saline and directed to waste vial. The product was then eluted with 1mL of 60% ethanol/water followed by 10mL saline and passed through a sterilizing filter. Typical yields range from 85 to 90% based on total ^{68}Ga eluted.

Animal Studies

Our prior data showing that upregulation of PSMA can be quantified with PET was demonstrated with ^{64}Cu-labeled J591. Since J591 is a full sized monoclonal antibody

with a long residence time in blood, it was not obvious that changes in PSMA could be measured with a more rapidly clearing agent like ^{68}Ga-PSMA-11. Therefore we measured relative changes in PSMA expression with ^{68}Ga-PSMA-11 in mice bearing LNCaP-AR xenografts. A total of twelve 3-5 week old male *nu/nu* mice obtained from Charles River were studied, four treated with vehicle, four with orchiectomy and four with Apalutamide (ARN-509), which is a non-steroideal competitive AR inhibitor. Mice were inoculated with 5 x 10^7 LnCAP-AR cells subcutaneously into one flank in a 1:1 mixture (vol/vol) of media and Matrigel (Corning). Tumors were palpable within 20-30 days after injection. Surgical castration was performed according to our Institutional Animal Care and Use Committee approved protocol under anesthesia with isoflurane. Separate treatment arms were treated with daily oral gavage of vehicle or ARN-509 (10 mg/kg/day) for seven days.

Small-Animal PET/CT

Positron Emission Tomography (PET) imaging was conducted using a Siemens Inveon microPET/Computed Tomography (CT) scanner at two time points, once before treatment and once seven days after treatment. Mice were injected with approximately 7.4 MBq of ^{68}Ga-PSMA via the tail-vein. One hour post injection, mice were anesthetized with 2% isoflurane and imaged for 10 to 20 min to acquire ~20 million coincident events. In the ARN-509 treated cohort, PET scans were timed at approximately 6 hours after the final gavage. Acquisitions were collected within an energy window of 350-650 keV and a coincidence-timing window of 3.432 ns. The data was converted into 2-dimentional histograms and images were reconstructed

by filter back-projection. After the PET acquisition, a co-registered CT scan was acquired within approximately 10 minutes. Mean Standardized Uptake Values (SUV_{mean}) were calculated for each xenograft using manually segmented regions of interest, and the ration of the SUV_{mean} after treatment to the SUV_{mean} before treatment was calculated for each animal.

Human experiments

This study was approved by the local institutional review board and informed consent was obtained from the patient. The patient was imaged at two time points, once prior to the initiation of ADT and a second time four weeks (29 days) after the initiation of ADT. He was imaged on a 3.0T GE Signa PET/Magnetic Resonance Imaging (MRI) (GE Healthcare, Waukesha, WI), and was injected with 207 ± 22 MBq of ^{68}Ga-PSMA-11, and PET/MRI began an average of 97 min after injection. A six bed-position whole body acquisition was performed from mid-thighs to vertex for 3 minutes at each bed position. PET data was reconstructed using a time-of-flight reconstruction with Ordered Subset Expectation Maximization using two iterations and 28 subsets, and a matrix size of 256 × 256. The PET transaxial and z-axis field of view are 600 and 250 mm, resulting in a voxel size of 2.3 × 2.3 mm. Axial slices were reconstructed at 2.78 mm in thickness. Attenuation correction was performed using a two-echo Dixon fat-water separation algorithm for the body while the lung was segmented using a region growing algorithm, which is standard on the scanner (*16*).

Patient image analysis

All segmentable lesions at both time points were segmented using a semi-automated method. For each lesion, the SUV_{max} was calculated. For lesions seen only on pre or post-therapy imaging, and volume of interest was placed in the same location as the other time point and the SUV_{max} was recorded. SUV_{peak} and SUV_{mean} were not calculated as many lesions were only seen on one time point, and therefore comparing SUV_{peak} and SUV_{mean} across two imaging studies was not feasible. All measurements were performed using an Advantage Workstation 5.0 (GE Healthcare).

Statistical analysis

A paired student's t-test was used to compare SUV_{max} before and after ADT in the patient and mouse xenografts. A non-paired student's t-test was used to compare the ratio of change in SUV_{mean} in mouse xenografts between treatment groups and vehicle.

RESULTS

Animal experiments

No change in tumor SUV_{mean} was observed in the group treated with vehicle (Fig. 1: ratio = 0.90 ± 0.14, p=0.85). Castration using orchiectomy resulted in an increase in SUV_{mean} (ratio = 1.55 ± 0.57, p=0.007). Treatment with ARN-509 resulted in the largest increase in SUV_{mean} (ration = 1.85 ± 0.44, p=0.013).

Human imaging

We imaged a 51 year-old man with Gleason 5+5 prostate cancer on biopsy, who had castration sensitive metastatic prostate cancer before and four weeks (29 days) after the initiation of ADT. The patient received no treatment before the first PSMA PET study. For ADT treatment, the patient received a single 7.5 mg intragluteal injection of leuprolide acetate (Lupron, AbbVie, Lakebluff, IL). The patient also received 50 mg of bicalutamide (Casodex, AstraZeneca, Wilmington, DE) daily for 30 days. His PSA decreased from 66.8 ng/mL to 9.0 ng/mL four weeks after the initiation of ADT. Imaging demonstrated an increase in ^{68}Ga-PSMA-11 uptake after the initiation of ADT (Fig. 2), with an increase in SUV_{max} across 22 measureable lesions from 2.9 ± 3.0 to 11.8 ± 6.9 resulting in a percent increase of 707 ± 689% ($p<0.001$). 13 of the 22 lesions were visible on PET only on post-ADT imaging, although these lesions in retrospect were present on MR imaging at the first time point (Fig 3).

DISCUSSION

We have reconfirmed that AR inhibition can increase PSMA expression in a mouse xenograft model using PSMA PET, and for the first time have shown that such an effect can be demonstrated in humans.

The increased uptake in the patient was seven-fold higher on the post-ADT imaging time point compared to pre-treatment imaging. These findings suggest that determining the optimal imaging time point after AR inhibition when PSMA expression is highest will be critical. Two processes are likely going on, first there is an increase in PSMA expression due to AR inhibition, as exhibited in our patient and

has been suggested recently using ^{99m}Tc-MIP-1404 PSMA.(17) Second, there is cell death due to therapeutic effect, which decreases the cell mass in the tumors reducing the overall PSMA uptake measured in the lesions. Previous work has shown that PSMA PET can image decreased tumor mass four months after treatment with ADT.(18) While over 80% of patients respond to ADT and chemical castration is typically achieved in 3-4 weeks,(15,19-21) the precise temporal relationship between initiation of ADT and PSMA expression is unknown, as is the variation in this relationship between individual patients. Further work to serially image patients after AR inhibition using ^{68}Ga-PSMA-11 is needed.

The temporal relationship between PSMA expression and initiation of ADT treatment may explain the different results in detection sensitivity of ^{68}Ga-PSMA-11 in biochemical recurrence patients. Afshar-Oromieh *et al* initially reported that detection sensitivity was increased in patients being treated with ADT (*8*), while Eiber *et al* did not demonstrate a difference in detection rate in patients treated with ADT (*7*). A third paper looked at a subpopulation of four patients with castration sensitive disease treated with ADT with falling PSAs, similar to our patient, and all four demonstrated positive disease on PSMA PET (*5*).

These findings have a number of important implications. If it is possible to upregulate PSMA expression in patients with prostate cancer by inhibiting the androgen receptor, then one could increase the detection sensitivity of metastases using PSMA PET in biochemical recurrence patients, which is supported by our results demonstrating 13 additional lesions were visualized on PSMA PET only after pretreatment with ADT. Additionally, one could increase the uptake of PSMA in

patients being treated with ^{177}Lu-PSMA (*22-24*). Groups have already demonstrated that PSMA targeted therapies can have increased efficacy when paired with AR targeted treatments (*25*). Additionally, one might be able to use changes in PSMA expression to interrogate the efficacy of second and third generation AR targeted therapies.

CONCLUSION

Inhibition of the androgen receptor can markedly change PSMA expression both in a mouse xenograft model as well as in clinical patients with castration sensitive prostate cancer when imaged using ^{68}Ga-PSMA-11.

CONFLICT OF INTEREST

TA Hope receives grant support and is on the speaker's bureau for GE Healthcare. MJ Evans receives consulting fees and owns shares in ORIC Pharmaceuticals, Inc. The authors have no other relevant affiliations or financial involvement with any organization or entity with a financial interest in or financial conflict with the subject matter or materials discussed in the manuscript apart from those disclosed.

REFERENCES

1. Israeli RS, Powell CT, Corr JG, Fair WR, Heston WD. Expression of the prostate-specific membrane antigen. Cancer Res. 1994;54:1807–1811.

2. Silver DA, Pellicer I, Fair WR, Heston WD, Cordon-Cardo C. Prostate-specific membrane antigen expression in normal and malignant human tissues. Clin Cancer Res. 1997;3:81–85.

3. Osborne JR, Akhtar NH, Vallabhajosula S, Anand A, Deh K, Tagawa ST. Prostate-specific membrane antigen-based imaging. Urol Oncol. 2013;31:144–154.

4. Hijazi S, Meller B, Leitsmann C, et al. Pelvic lymph node dissection for nodal oligometastatic prostate cancer detected by 68Ga-PSMA-positron emission tomography/computerized tomography. Prostate. 2015;75:1934–1940.

5. Ceci F, Uprimny C, Nilica B, et al. (68)Ga-PSMA PET/CT for restaging recurrent prostate cancer: which factors are associated with PET/CT detection rate? Eur J Nucl Med Mol Imaging. 2015;42:1284–1294.

6. Morigi JJ, Stricker PD, van Leeuwen PJ, et al. Prospective comparison of 18F-fluoromethylcholine versus 68Ga-PSMA PET/CT in prostate cancer patients who have rising PSA after curative treatment and are being considered for targeted therapy. J Nucl Med. 2015;56:1185–1190.

7. Eiber M, Maurer T, Souvatzoglou M, et al. Evaluation of Hybrid ^{68}Ga-PSMA Ligand PET/CT in 248 Patients with biochemical recurrence after radical prostatectomy. J Nucl Med. 2015;56:668–674.

8. Afshar-Oromieh A, Avtzi E, Giesel FL, et al. The diagnostic value of PET/CT imaging with the (68)Ga-labelled PSMA ligand HBED-CC in the diagnosis of recurrent prostate cancer. Eur J Nucl Med Mol Imaging. 2015;42:197–209.

9. Afshar-Oromieh A, Malcher A, Eder M, et al. PET imaging with a [68Ga]gallium-labelled PSMA ligand for the diagnosis of prostate cancer: biodistribution in humans and first evaluation of tumour lesions. Eur J Nucl Med Mol Imaging. 2012;40:486–495.

10. Evans MJ. Measuring oncogenic signaling pathways in cancer with PET: an emerging paradigm from studies in castration-resistant prostate cancer. Cancer Discov. 2012;2:985–994.

11. Evans MJ, Smith-Jones PM, Wongvipat J, et al. Noninvasive measurement of androgen receptor signaling with a positron-emitting radiopharmaceutical that targets prostate-specific membrane antigen. Proc Natl Acad Sci USA. 2011;108:9578–9582.

12. Wright GL, Grob BM, Haley C, et al. Upregulation of prostate-specific membrane antigen after androgen-deprivation therapy. Urology. 1996;48:326–334.

13. Meller B, Bremmer F, Sahlmann CO, et al. Alterations in androgen deprivation enhanced prostate-specific membrane antigen (PSMA) expression in prostate cancer cells as a target for diagnostics and therapy. EJNMMI Res. 2015;5:66.

14. Miyamoto DT, Lee RJ, Stott SL, et al. Androgen receptor signaling in circulating tumor cells as a marker of hormonally responsive prostate cancer. Cancer Discov. 2012;2:995–1003.

15. Hussain M, Tangen CM, Higano C, et al. Absolute prostate-specific antigen value after androgen deprivation is a strong independent predictor of survival in new metastatic prostate cancer: data from Southwest Oncology Group Trial 9346 (INT-0162). J Clin Oncol. 2006;24:3984–3990.

16. Wollenweber SD, Ambwani S. Comparison of 4-class and continuous fat/water methods for whole-body, MR-based PET attenuation correction. Nuclear Science. 2013.

17. Vallabhajosula S, Jhanwar Y, Tagawa S, et al. 99mTc-MIP-1404 Planar and SPECT scan: Imaging biomarker of androgen receptor (AR) signaling and prostate specific membrane antigen (PSMA) expression. Journal of Nuclear Medicine. 2016;57:1541–1541.

18. Schlenkhoff CD, Gaertner F, Essler M, Hauser S, Ahmadzadehfar H. 68Ga-labeled anti-prostate-specific membrane antigen peptide as marker for androgen deprivation therapy response in prostate cancer. Clin Nucl Med. 2016;41:423–425.

19. Seidenfeld J, Samson DJ, Hasselblad V, et al. Single-therapy androgen suppression in men with advanced prostate cancer: a systematic review and meta-analysis. Ann Intern Med. 2000;132:566–577.

20. Miyamoto H, Messing EM, Chang C. Androgen deprivation therapy for prostate cancer: current status and future prospects. Prostate. 2004;61:332–353.

21. Sharifi N, Gulley JL, Dahut WL. Androgen deprivation therapy for prostate cancer. JAMA. 2005;294:238–244.

22. Baum RP, Kulkarni HR, Schuchardt C, et al. 177Lu-labeled prostate-specific membrane antigen radioligand therapy of metastatic castration-resistant prostate cancer: safety and efficacy. J Nucl Med. 2016;57:1006–1013.

23. Zechmann CM, Afshar-Oromieh A, Armor T, et al. Radiation dosimetry and first therapy results with a (124)I/ (131)I-labeled small molecule (MIP-1095)

targeting PSMA for prostate cancer therapy. Eur J Nucl Med Mol Imaging. 2014;41:1280–1292.

24. Kratochwil C, Giesel FL, Stefanova M, et al. PSMA-targeted radionuclide therapy of metastatic castration-resistant prostate cancer with Lu-177 labeled PSMA-617. J Nucl Med. 2016.

25. DiPippo VA, Nguyen HM, Brown LG, Olson WC, Vessella RL, Corey E. Addition of PSMA ADC to enzalutamide therapy significantly improves survival in in vivo model of castration resistant prostate cancer. Prostate. 2016;76:325–334.

FIGURES

Figure 1: ^{68}Ga-PSMA-11 PET demonstrates increased PSMA expression in prostate cancer xenografts with inhibition of the androgen receptor. The ratio of SUV_{mean} at day 7 to day 0 increased an average of 72% with orchiectomy and 105% with ARN-509 compared to vehicle (A, * p=0 .07, ** p=0.006). Visual assessment of the ^{68}Ga-PSMA-11 PET demonstrates a clear increase in uptake in the xenografts in response to ARN-509 (B, middle row) and orchiectomy (B, bottom row), compared to controls treated with vehicle (B, top row).

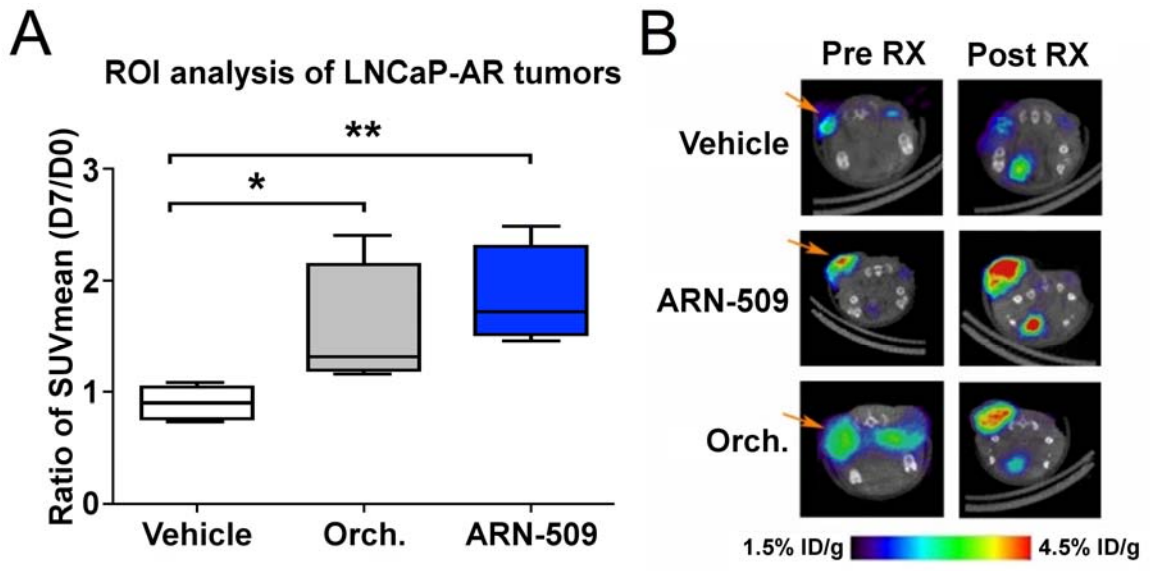

Figure 2: Coronal MIP images of a patient with castration sensitive metastatic prostate cancer imaged using ^{68}Ga-PSMA-11 before ADT (A) and after ADT (B) demonstrate a marked increase in uptake in the lesions. Each lesion visualized demonstrated an increase up, with an average increase of over 7 times the initial uptake (C). Numerous lesions (13 of 22 lesions) were only visualized on post-treatment imaging, for example an upper thoracic osseous metastases (axial PET images of lesion 1, D and E). Other lesions increased in size and had increased uptake compared to pre-ADT imaging (axial PET images of lesions 2, F and G).

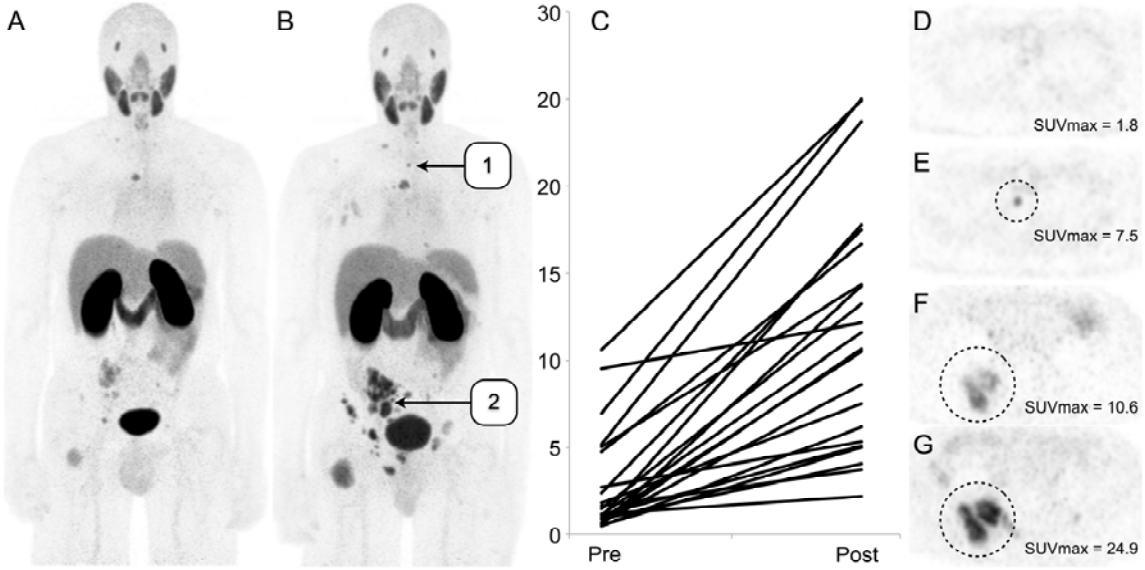

Figure 3: Example lesion seen only on post-ADT PSMA PET. Pre-treatment PET (A and B) demonstrates a single lesion in the right acetabulum (B, black circle). An additional lesion right acetabulum lesion is is seen on the same MR image just lateral to the larger lesion (A, red arrow), which does not demonstrate PSMA avidity. On post-ADT PET (C and D), numerous additional lesions are seen on the PET including the adjacent acetabular lesion (D, red arrow), which are again demonstrated on post-contrast T1-weighted images (C, red arrow).